

## Article

# Hydrogen Generation by Hydrolysis of MgH<sub>2</sub>-LiH Composite

Xiaojuan Wu <sup>1,2</sup>, Huaqing Xue <sup>3</sup>, Yong Peng <sup>3</sup>, Jifeng Deng <sup>1,2</sup>, Zewei Xie <sup>1,2</sup>, Jie Zheng <sup>1,2</sup>, Xingguo Li <sup>1,2</sup>  
and Shuan Li <sup>1,2,\*</sup>

<sup>1</sup> Beijing National Laboratory for Molecular Sciences, College of Chemistry and Molecular Engineering, Peking University, Beijing 100871, China; xiaojuanwu@pku.edu.cn (X.W.); jfdeng@pku.edu.cn (J.D.); zwxie@pku.edu.cn (Z.X.); zhengjie@pku.edu.cn (J.Z.); xgli@pku.edu.cn (X.L.)

<sup>2</sup> State Key Laboratory of Rare Earth Materials Chemistry and Applications, College of Chemistry and Molecular Engineering, Peking University, Beijing 100871, China

<sup>3</sup> Research Center of New Energy, Research Institute of Petroleum Exploration & Development, Beijing 100083, China; hqxue@petrochina.com.cn (H.X.); pengyong13@petrochina.com.cn (Y.P.)

\* Correspondence: lishuan@pku.edu.cn

**Abstract:** As a most promising material for hydrogen generation by hydrolysis, magnesium hydride (MgH<sub>2</sub>) is also trapped by its yielded byproduct Mg(OH)<sub>2</sub> whose dense passivated layers prevent the further contact of intimal MgH<sub>2</sub> with water. In this work, LiH, as a destroyer, has been added to promote the hydrogen properties of MgH<sub>2</sub>. The results demonstrate that even 3 wt % LiH was added into MgH<sub>2</sub>-G, the hydrogen generation yield can increase about 72% compared to the hydrogen generation yield of MgH<sub>2</sub>-G. The possible mechanism is that Mg<sup>2+</sup> from the hydrolysis of MgH<sub>2</sub> preferentially bound with OH<sup>-</sup> ions from the hydrolysis of LiH to form Mg(OH)<sub>2</sub> precipitation, which is dispersed in water rather than coated on the surface of MgH<sub>2</sub>. Moreover, adding MgCl<sub>2</sub> into hydrolysis solution, using ball milling technology, and increasing the hydrolysis temperature can make the hydrolysis rate higher and reaction process more complete. It is noted that a too high weight ratio of LiH with too high of a hydrolysis temperature will make the reaction too violent to be safe in the experiment. We determinate the best experimental condition is that the LiH ratio added into MgH<sub>2</sub> is 3 wt %, the hydrolysis temperature is 60 °C, and the concentration of MgCl<sub>2</sub> hydrating solution is 1 M. MgH<sub>2</sub>-LiH composite hydrogen generation technology can meet the needs of various types of hydrogen supply and has broad application prospects.

**Keywords:** MgH<sub>2</sub>-LiH composite; ball milling; hydrogen generation; bath temperatures; MgCl<sub>2</sub> aqueous solution



**Citation:** Wu, X.; Xue, H.; Peng, Y.; Deng, J.; Xie, Z.; Zheng, J.; Li, X.; Li, S. Hydrogen Generation by Hydrolysis of MgH<sub>2</sub>-LiH Composite. *Materials* **2022**, *15*, 1593. <https://doi.org/10.3390/ma15041593>

Academic Editor: Karol J. Fijałkowski

Received: 22 November 2021

Accepted: 23 December 2021

Published: 21 February 2022

**Publisher's Note:** MDPI stays neutral with regard to jurisdictional claims in published maps and institutional affiliations.



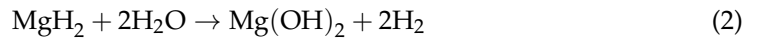
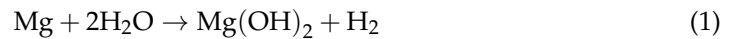
**Copyright:** © 2022 by the authors. Licensee MDPI, Basel, Switzerland. This article is an open access article distributed under the terms and conditions of the Creative Commons Attribution (CC BY) license (<https://creativecommons.org/licenses/by/4.0/>).

## 1. Introduction

Currently, the contradiction between the decreasing of global fossil energy and the infinite demand for energy is the main factor that restricts the sustainable development of society [1,2]. Hydrogen energy is considered to be the most potential energy carrier for replacing traditional fossil fuels in the future because of its advantages such as abundant reserves, high energy density (142 MJ/kg), environmental protection, and renewability [3–6]. Hydrogen fuel cell is the most attractive new energy, and its “fuel” is hydrogen, so efficient and safe hydrogen generation technology is particularly important [7]. Hydrogen generation by hydrolysis is a kind of on-site hydrogen generation method, which can be easily applied to various mobile devices [8–10].

At present, scientists have paid their attention into the hydrogen generation by the hydrolysis of metal or metal hydrides and chemical hydrides, such as MgH<sub>2</sub>, NaBH<sub>4</sub>, CaH<sub>2</sub>, and LiH, and their theoretical hydrogen yield of are 15.32 wt %, 21.32 wt %, 9.58 wt %, and 25.36 wt % (without H<sub>2</sub>O), respectively. NaBH<sub>4</sub> is considered as a promising hydrogen storage material; however, NaBH<sub>4</sub> needs noble catalysts to improve the kinetic performance of hydrolysis, and high cost of recovery of byproducts [11–13], while CaH<sub>2</sub> and LiH all react violently with water, making it difficult to control the course of experiments [14,15].

By comparison, MgH<sub>2</sub> has not only a high theoretical hydrogen generation but also environmentally friendly hydrolysis byproduct Mg(OH)<sub>2</sub>, what is more, the hydrolysis of Mg-based materials is considered as a clean hydrogen generation technique and Mg element is abundant on Earth [16]. MgH<sub>2</sub> has a lower cost than other hydrolyzed materials, which is regarded the most promising hydrolysis of material. The reaction equations are as follows:



However, the dense passivation layer of Mg(OH)<sub>2</sub> will prevent the further contact of water with intimal MgH<sub>2</sub>, which results in sluggish hydrolysis kinetics [17,18]. In the process of hydrolysis, in order to remove the passivation layer and promote the hydrolysis reaction of MgH<sub>2</sub>, researchers have made great efforts, such as the introduction of various cations/anions in the solution [19–21], the addition of additives [21–23], alloying [16,24–27], reduce Mg particle size [28], and so on. These methods play an important role in improving the hydrolysis kinetics and hydrogen generation capacity to a certain extent.

In this paper, to improve the hydrolysis properties of MgH<sub>2</sub>, we choose the LiH with high hydrogen storage capacity and light weight to add into MgH<sub>2</sub>. The effects of milling technology, solution, water solution temperature, and the amount of adding LiH on the hydrolysis performance of MgH<sub>2</sub> were studied.

## 2. Experimental Details

### 2.1. Sample Preparation

The Mg powder was prepared by the hydrogen plasma metal reaction (HPMR), the detailed description is given in the published article [29]. Then, the Mg powder was placed in a steel reactor which vacuum to 10<sup>−3</sup> Pa, and heated to 400 °C for 5 h, followed by hydrogenation under 4 MPa hydrogen atmosphere at 673 K for 10 h. Finally, the reactor was vacuumed, and the sample was taken out to obtain the MgH<sub>2</sub>. The MgH<sub>2</sub> and LiH powders were mixed in different mass ratios by obtained by planetary ball milling (BM) and by grinding (G) in agate mortar, respectively, which operated in the argon atmosphere glove box. The LiH was purchased from Alfa Aesar (Lancashire, UK), there is no further purification.

The phase composition of the samples was determined by a powder X-ray diffraction (XRD) method. The XRD patterns were obtained on an X-Pert3 powder diffractometer (PANalytical, Almelo, The Netherlands) in the 2θ range from 5° to 80° using the CuKα radiation. The morphologies of the samples were observed using a JSM-IT300 (JEOL, Tokyo, Japan) scanning electron microscopy (SEM).

### 2.2. Hydrolysis Experiment

The hydrolysis reactions were tested on a self-assembled system in room temperature. The 50 mg of sample was added into the flask with three opening in the glove box and take out the glove box and quickly connect it to the test system. Then 50 mL of 1 M MgCl<sub>2</sub> aqueous solution was injected into the conical flask with a syringe. After opening the peristaltic pump, MgCl<sub>2</sub> aqueous solution dropped in the three-mouth flask, and the hydrogen was collected by draining water gathering of gas law and recorded the volume of discharged water.

## 3. Results and Discussion

Figure 1a shows the hydrogen generation curves of MgH<sub>2</sub>-G and MgH<sub>2</sub>-3 wt % LiH-G in deionized water. As shown in Figure 1a, the hydrogen yield of the MgH<sub>2</sub>-G and MgH<sub>2</sub>-3 wt % LiH-G are about 130 mL/g, and 230 mL/g, respectively. Although the hydrogen generation yield of MgH<sub>2</sub>-3 wt % LiH-G and MgH<sub>2</sub>-G are only about 10% of their theoretical value, respectively, the hydrogen generation yield of MgH<sub>2</sub>-3 wt % LiH-G

increase about 72% compared to the hydrogen generation yield of  $\text{MgH}_2\text{-G}$ . At the same time, from Figure 1b, the hydrolysis byproducts mainly contain a major phase unreacted  $\text{MgH}_2$  and a secondary phase  $\text{Mg}(\text{OH})_2$ . The XRD results indicate that the  $\text{Mg}(\text{OH})_2$  layer formed on the surface samples hindered the hydrolysis reaction. However, it also shows that the LiH addition increased the hydrogen yield properties.

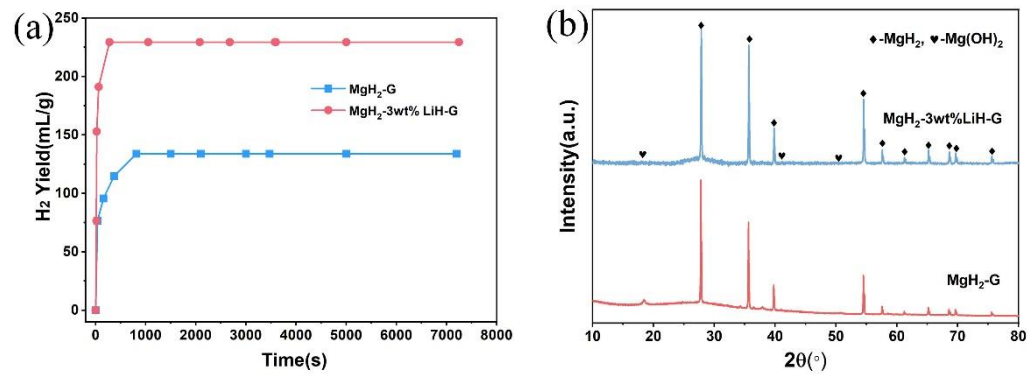


**Figure 1.** (a) The hydrogen generation curves and (b) XRD patterns of the hydrolysis byproduct of  $\text{MgH}_2\text{-G}$  and  $\text{MgH}_2\text{-3 wt % LiH-G}$ .

In order to improve the hydrogen yield, adding a small amount of  $\text{MgCl}_2$  is a common way to promote the hydrolysis of  $\text{MgH}_2$ . Figure 2a,b are the hydrogen yield and the hydrogen generation rate of the  $\text{MgH}_2\text{-3 wt % LiH-G}$  in the different concentrations (0, 0.1, 0.5, 1) of  $\text{MgCl}_2$  aqueous solution, respectively. As shown in Figure 2a, the hydrogen yield curves in 0.1 M, 0.5 M, and 1 M  $\text{MgCl}_2$  solutions are compared. The hydrogen production rate diagram from Figure 2b is converted from the data in Figure 2a. The results indicate that  $\text{MgCl}_2$  aqueous solution is beneficial for improvement of the  $\text{MgH}_2\text{-3 wt % LiH}$  hydrolysis; their hydrolysis reaction is relatively complete, almost 100%. In addition, in the 1M  $\text{MgCl}_2$  aqueous solution, the sample has the fastest hydrolysis rate. The result is consistent with XRD results from Figure 3. The hydrolysis byproduct mainly contains  $\text{Mg}(\text{OH})_2$ ; unreacted  $\text{MgH}_2$  is not found.

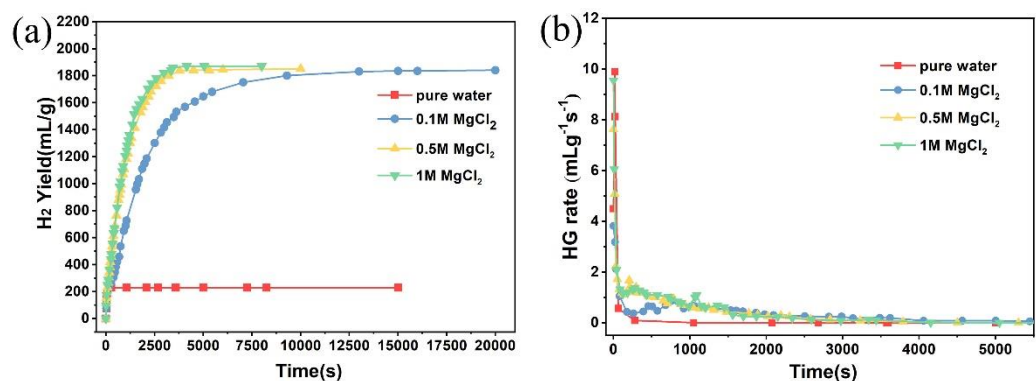


**Figure 2.** (a) The hydrogen generation curves and (b) hydrogen generation rate and hydrolysis by-product XRD patterns of  $\text{MgH}_2\text{-3 wt % LiH-G}$  in 0.1 M, 0.5 M and 1 M  $\text{MgCl}_2$  solutions.

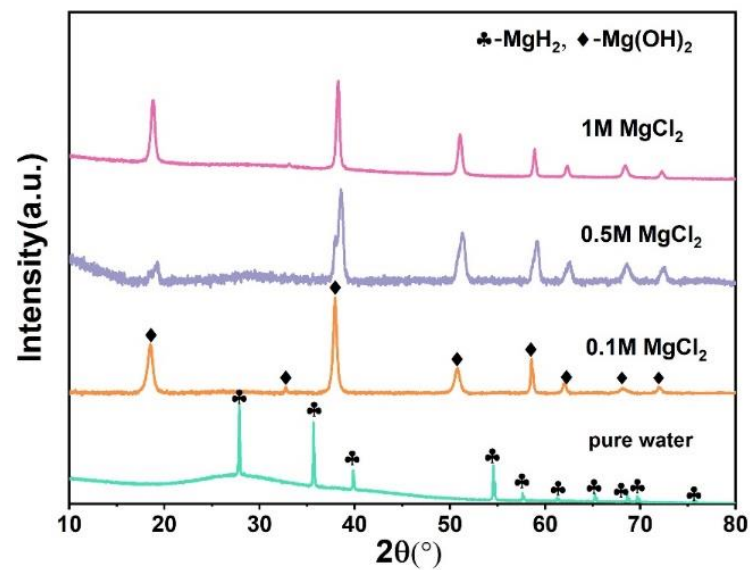


**Figure 3.** XRD patterns of the hydrolysis by-products of  $\text{MgH}_2$ -3wt %LiH-G in the different concentrations of  $\text{MgCl}_2$  aqueous solution.

In order to obtain the effect of LiH on  $\text{MgH}_2$ -LiH system, we tested the hydrogen generation yield and hydrogen generation rate of  $\text{MgH}_2$  with the different amounts of LiH, as shown in Figure 4a,b, respectively. From Figure 4a, the  $\text{MgH}_2$ -G,  $\text{MgH}_2$ -1.5 wt % LiH-G, and  $\text{MgH}_2$ -3 wt % LiH-G generated 1753 mL/g, 1840 mL/g, and 1870 mL/g hydrogen, respectively. Obviously, the addition of LiH improves the hydrogen yield. Furthermore, we can see that the hydrogen generation rate is also improved in Figure 4b. The results indicate the addition of LiH not only enhance hydrogen generation yield but also increase hydrogen generation rate. The mechanism of the reaction will be described later in this paper.

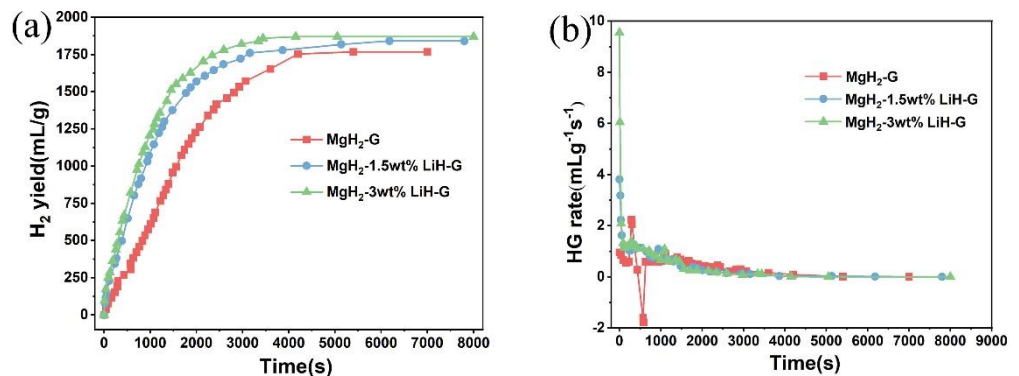


**Figure 4.** (a) Hydrogen generation curves and (b) hydrogen generation rate of  $\text{MgH}_2$ -G,  $\text{MgH}_2$ -1.5 wt % LiH-G, and  $\text{MgH}_2$ -3 wt % LiH-G.

Figure 5 shows the XRD pattern of  $\text{MgH}_2$ -3 wt % LiH-BM and  $\text{MgH}_2$ -3 wt % LiH-G. We compared the hydrolytic properties of  $\text{MgH}_2$ -3 wt % LiH-BM and  $\text{MgH}_2$ -3 wt % LiH-G. The two samples were composed of  $\text{MgH}_2$  and LiH, in addition, small peaks of MgO and LiOH could also be observed. This MgO is introduced during preparation and LiOH is introduced XRD characterization process.

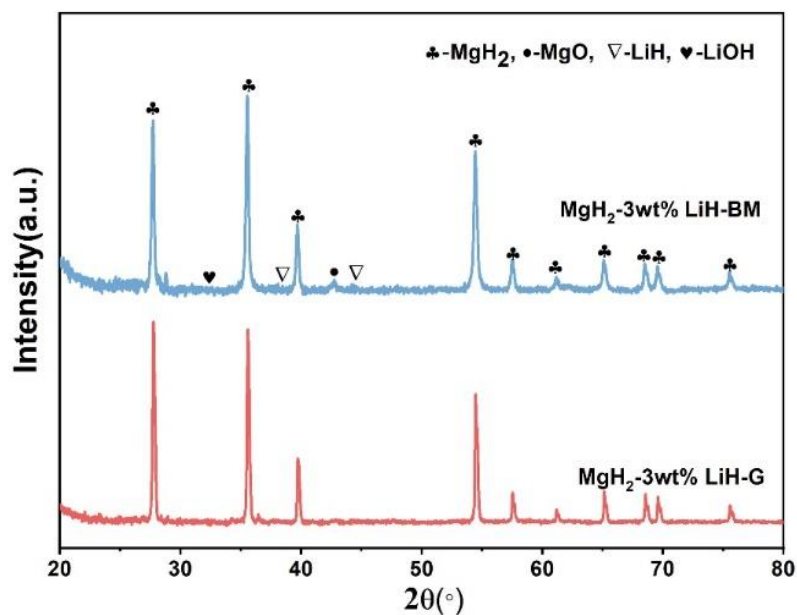


Figure 5. XRD patterns of the hydrolysis byproduct of  $\text{MgH}_2$ -3 wt % LiH-BM and  $\text{MgH}_2$ -3 wt % LiH-G.

Figure 6a,b show the hydrogen generation curves and hydrogen generation rate of  $\text{MgH}_2$ -3 wt % LiH-BM and  $\text{MgH}_2$ -3 wt % LiH-G, respectively. It can be seen that the  $\text{MgH}_2$ -3 wt % LiH-BM can generate about 1830 mL/g in 800 s, continue to generate hydrogen until 1890 mL/g in 1500 s, which can close to the maximum hydrogen yield for the studied samples. The  $\text{MgH}_2$ -3 wt % LiH-G can generate 1820 mL/g in 3000 s. Finally, the maximum value is reached more than 3500 s. Obviously, the  $\text{MgH}_2$ -3 wt % LiH-BM exhibits a higher hydrogen generation rate than the  $\text{MgH}_2$ -3 wt % LiH-G. From the above experimental results, the ball milling in a short time plays an important role in increasing the rate of hydrogen generation. The results should be closely related to the particle size of the sample. In order to provide more direct experimental evidence, the SEM images of the two samples are given in Figure 7. From the SEM images of the two samples, we can see that the  $\text{MgH}_2$ -3 wt % LiH-BM are obviously smaller than the  $\text{MgH}_2$ -3 wt % LiH-G, proving the above hydrogen generation properties analysis results of two samples.

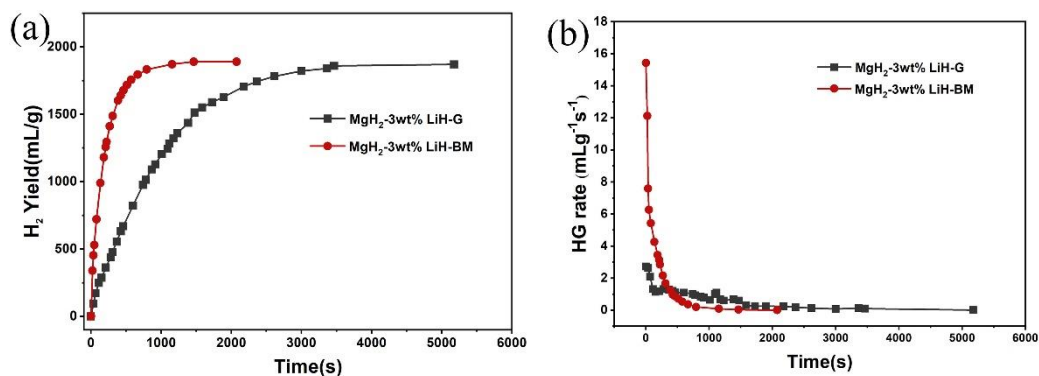
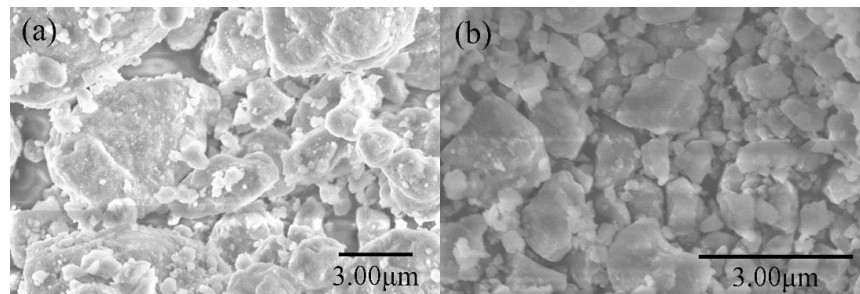
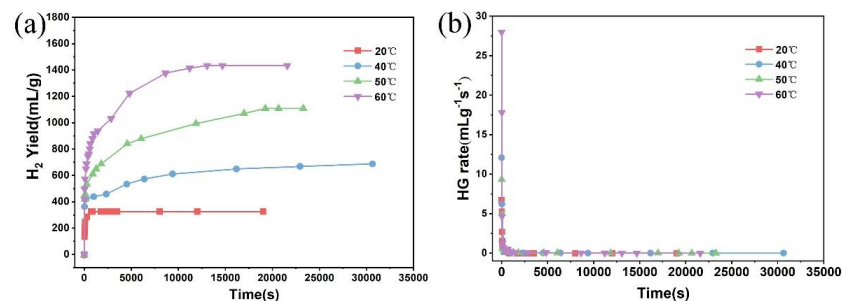


Figure 6. (a) Hydrogen generation curves and (b) hydrogen generation rate of  $\text{MgH}_2$ -3 wt % LiH-BM and  $\text{MgH}_2$ -3 wt % LiH-G.



**Figure 7.** (a) SEM of MgH<sub>2</sub>-3 wt % LiH-G and (b) MgH<sub>2</sub>-3 wt % LiH-BM.

Furthermore, in order to study the hydrolysis properties of the sample in deionized water, the MgH<sub>2</sub>-3 wt % LiH-BM in deionized water at the different water bath temperatures were investigated as shown in Figure 8. The hydrogen generation yield and hydrogen generation rate are enhanced with the increase of water bath temperatures. One possible reason is that the higher temperature is conducive to the dissolution of Mg(OH)<sub>2</sub>. Figure 9 shows XRD patterns of the byproducts after hydrolysis in deionized water at water bath temperatures with 50 °C and 60 °C. From Figure 9, the byproducts are composed of MgH<sub>2</sub>, Mg(OH)<sub>2</sub>, and Li<sub>2</sub>CO<sub>3</sub>. In the byproducts, Li<sub>2</sub>CO<sub>3</sub> may come from CO<sub>2</sub> absorbed by the LiOH byproduct during the drying and testing process. LiOH is dissolved in water, so there is no associated diffraction peak in XRD [26]. According to the XRD results, the reaction of Mg, MgH<sub>2</sub> and LiH could be described as follow:



**Figure 8.** (a) Hydrogen generation curves and (b) hydrogen generation rate of the MgH<sub>2</sub>-3 wt % LiH-BM in water at different bath temperatures.

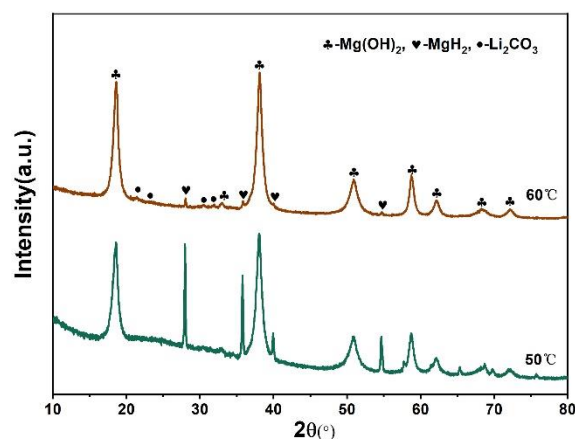


**Figure 9.** XRD patterns of the hydrolysis byproducts of MgH<sub>2</sub>-3 wt % LiH-BM in deionized water at different bath temperatures.

As the water bath temperature increases from 50 °C to 60 °C, the diffraction peaks intensity of  $\text{Mg}(\text{OH})_2$  increases while the intensity of  $\text{MgH}_2$  decreases. The hydrolysis properties of the sample is obviously dependent on temperature [30]. When the water bath temperature is 60 °C, the final hydrolysis yield reaches about 1510 mL/g until 250 min, with the conversion rate up to about 80%. These results also prove that the suitable water temperature is beneficial to the hydrolysis reaction.

We carefully compared hydrogen generation of the  $\text{MgH}_2$ -BM and  $\text{MgH}_2$ -3 wt % LiH-BM at 60 °C in Figure 10a. As can be seen, the hydrogen generation rate of  $\text{MgH}_2$ -3 wt % LiH-BM is improved. The presence of LiH can increase the hydrolysis rate compared to pure  $\text{MgH}_2$ . The result can also be seen visually from the hydrogen generation rate diagram, as shown in Figure 10b.

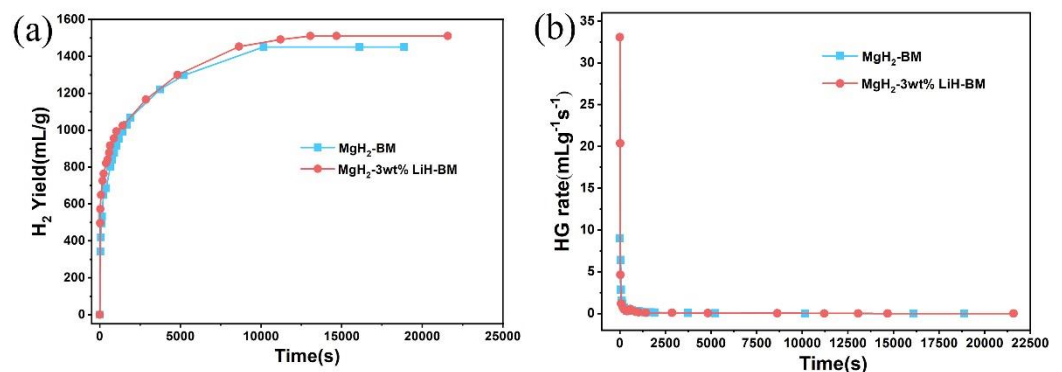


**Figure 10.** (a) Hydrogen generation curves and (b) hydrogen generation rate of the  $\text{MgH}_2$  and  $\text{MgH}_2$ -3 wt % LiH-BM in water at 60 °C.

The possible hydrolysis mechanism of the  $\text{MgH}_2$ -LiH system in  $\text{MgCl}_2$  aqueous solution was detailed described in previous work of our research group [21]. In pure water, the  $\text{MgH}_2$  hydrolysis reaction leads to an increase  $-\text{OH}$  concentration on the particles surface. The precipitation of  $-\text{OH}$  and  $\text{Mg}^{2+}$  mainly occurs on the surface of particles, so the byproduct  $\text{Mg}(\text{OH})_2$  rapidly deposits on the surface of particles, forming a dense passivation layer. The passivation layer prevents further hydrolysis of  $\text{MgH}_2$ . In  $\text{MgCl}_2$  aqueous solution, due to the presence of a large amount of  $\text{Mg}^{2+}$  in the whole solution system, the  $\text{Mg}^{2+}$  in solution competes with the  $\text{MgH}_2$  on the surface during the formation of  $\text{Mg}(\text{OH})_2$  precipitation, that is to say,  $\text{Mg}^{2+}$  in solution combine with  $\text{OH}^-$  on the surface of  $\text{MgH}_2$ . In this case, the resulting precipitate is dispersed in the solution rather than forming a passivated layer on the surface.

For hydrolysis properties of the  $\text{MgH}_2$ -3 wt % LiH-BM and  $\text{MgH}_2$ -3 wt % LiH-G, the  $\text{MgH}_2$ -3 wt % LiH-BM has better hydrolysis kinetics than  $\text{MgH}_2$ -3 wt % LiH-G. This result is that the reduction of particle size of the samples after planetary ball milling cause the larger specific surface area of the samples, which is more conducive to the rapid hydrolysis reaction [23,30].

For the role of LiH, by XRD, SEM, and reaction byproduct analysis, LiH is uniformly attached to the surface of  $\text{MgH}_2$ . LiH hydrolyzes rapidly in water, and the reaction equation is shown as (3):  $\text{LiH} + \text{H}_2\text{O} \rightarrow \text{LiOH} + \text{H}_2$ . Then,  $\text{Mg}^{2+}$  preferentially binds with  $\text{OH}^-$  ions to form  $\text{Mg}(\text{OH})_2$  precipitation, which is dispersed in water rather than coated on the surface of  $\text{MgH}_2$  nanoparticles. The result is in agreement with reported results for MgLi alloy and  $\text{MgH}_2$ - $\text{LiNH}_2$  composites [8,26].

In addition, in the process of planetary ball milling and grinding in agate mortar, LiH will also enter between  $\text{MgH}_2$  nanoparticles to disperse  $\text{MgH}_2$  and conduce to  $\text{MgH}_2$  fully contact with aqueous solution.

#### 4. Conclusions

In this work, the hydrolysis properties of the MgH<sub>2</sub>-LiH system have been studied. The 3 wt % LiH is added into MgH<sub>2</sub>, the hydrogen generation yield can increase about 72% compared to the hydrogen generation yield of MgH<sub>2</sub>-G. The MgH<sub>2</sub>-LiH system hydrolysis is relatively complete, almost 100%, also has the fastest hydrolysis rate in the 1M MgCl<sub>2</sub> aqueous solution. In a short time, the ball milling reduces the particle size of the samples and cause the larger specific surface area of the samples, which is more conducive to the rapid hydrolysis reaction. The higher water solution temperature is helpful to improve the hydrolysis properties. When the water bath temperature is 60 °C, the final hydrolysis yield reaches to about 1510 mL/g until 250 min.

**Author Contributions:** Conceptualization, X.W., H.X., Y.P., Z.X., J.Z., X.L. and S.L.; Data curation, X.W.; Formal analysis, X.W., H.X., Y.P., J.D. and Z.X.; Funding acquisition, X.L. and S.L.; Investigation, X.W., J.D. and S.L.; Methodology, X.W., J.D., Z.X. and J.Z.; Project administration, X.L. and S.L.; Resources, H.X., J.D. and J.Z.; Supervision, H.X., Y.P., J.Z. and X.L.; Validation, X.W. and Z.X.; Visualization, X.W.; Writing—original draft, X.W.; Writing—review & editing, X.W. and S.L. All authors have read and agreed to the published version of the manuscript.

**Funding:** This research was funded by China Postdoctoral Science Foundation (No. BX20200004), MOST of China (No. 2018YFB1502102) and NSFC (No. 51971004 and 51771002).

**Institutional Review Board Statement:** Not applicable.

**Informed Consent Statement:** Not applicable.

**Data Availability Statement:** Not applicable.

**Conflicts of Interest:** The authors declare no conflict of interest.

#### References

1. Shao, H.; He, L.; Lin, H.; Li, H.W. Progress and trends in magnesium-based materials for energy-storage research: A review. *Energy Technol.* **2018**, *6*, 445–458. [[CrossRef](#)]
2. Rusman, N.A.A.; Dahari, M. A review on the current progress of metal hydrides material for solid-state hydrogen storage applications. *Int. J. Hydrog. Energy* **2016**, *41*, 12108–12126. [[CrossRef](#)]
3. Sakintuna, B.; Lamaridarkrim, F.; Hirscher, M. Metal hydride materials for solid hydrogen storage: A review. *Int. J. Hydrog. Energy* **2007**, *32*, 1121–1140. [[CrossRef](#)]
4. He, T.; Pachfule, P.; Wu, H.; Xu, Q.; Chen, P. Hydrogen carriers. *Nat. Rev. Mater.* **2016**, *1*, 16059. [[CrossRef](#)]
5. Badea, N.I. Hydrogen as energy sources-basic concepts. *Energies* **2021**, *14*, 5783. [[CrossRef](#)]
6. Deng, J.F.; Chen, S.P.; Wu, X.J.; Zheng, J.; Li, X.G. Recent progress on materials for hydrogen generation via hydrolysis. *J. Inorg. Mater.* **2021**, *36*, 1–8.
7. Olabi, A.G.; Bahri, A.S.; Abdelghafar, A.A.; Baroutaji, A.; Sayed, E.T.; Alami, A.H.; Rezk, H.; Abdelkareem, M.A. Large-scale hydrogen production and storage technologies: Current status and future directions. *Int. J. Hydrog. Energy* **2021**, *46*, 23498–23528. [[CrossRef](#)]
8. Ma, M.; Ouyang, L.; Liu, J.; Wang, H.; Shao, H.; Zhu, M. Air-stable hydrogen generation materials and enhanced hydrolysis performance of MgH<sub>2</sub>-LiNH<sub>2</sub> composites. *J. Power Sources* **2017**, *359*, 427–434. [[CrossRef](#)]
9. Wei, Y.; Wang, M.; Fu, W.; Wei, L.; Zhao, X.; Zhou, X.; Ni, M.; Wang, H. Highly active and durable catalyst for hydrogen generation by the NaBH<sub>4</sub> hydrolysis reaction: CoWB/NF nanodendrite with an acicular array structure. *J. Alloys Compd.* **2020**, *836*, 155429. [[CrossRef](#)]
10. Huang, C.; Yu, Y.; Tang, X.; Liu, Z.; Zhang, J.; Ye, C.; Ye, Y.; Zhang, R. Hydrogen generation by ammonia decomposition over Co/CeO<sub>2</sub> catalyst: Influence of support morphologies. *Appl. Surf. Sci.* **2020**, *532*, 147335. [[CrossRef](#)]
11. Lei, W.; Jin, H.; Gao, J.; Chen, Y. Efficient hydrogen generation from the NaBH<sub>4</sub> hydrolysis by amorphous Co-Mo-B alloy supported on reduced graphene oxide. *J. Mater. Res.* **2021**, *36*, 4154–4168. [[CrossRef](#)]
12. Li, Z.; Xu, Y.; Guo, Q.; Li, Y.; Ma, X.; Li, B.; Zhu, H.; Yuan, C.G. Preparation of Ag@PNCMs nanocomposite as an effective catalyst for hydrogen generation from hydrolysis of sodium borohydride. *Mater. Lett.* **2021**, *297*, 129828. [[CrossRef](#)]
13. Deng, J.; Sun, B.; Xu, J.; Shi, Y.; Xie, L.; Zheng, J.; Li, X. A monolithic sponge catalyst for hydrogen generation from sodium borohydride solution for portable fuel cells. *Inorg. Chem. Front.* **2021**, *8*, 35–40. [[CrossRef](#)]
14. Figen, A.K.; Taşçı, K. Hydrolysis characteristics of calcium hydride (CaH<sub>2</sub>) powder in the presence of ethylene glycol, methanol, and ethanol for controllable hydrogen production. *Energy Sources Part A Recovery Util. Environ. Eff.* **2016**, *38*, 37–42. [[CrossRef](#)]
15. Khzouz, M.; Gkanas, E.I.; Girella, A.; Statheros, T.; Milanese, C. Sustainable hydrogen production via LiH hydrolysis for unmanned air vehicle (UAV) applications. *Int. J. Hydrog. Energy* **2020**, *45*, 5384–5394. [[CrossRef](#)]

16. Hou, X.; Wang, Y.; Yang, Y.; Hu, R.; Yang, G.; Feng, L.; Suo, G.; Ye, X.; Zhang, L.; Shi, H.; et al. Enhanced hydrogen generation behaviors and hydrolysis thermodynamics of as-cast Mg-Ni-Ce magnesium-rich alloys in simulate seawater. *Int. J. Hydrog. Energy* **2019**, *44*, 24086–24097. [[CrossRef](#)]
17. Zhou, C.; Zhang, J.; Liu, J.; Shi, R.; Zhu, Y.; Liu, Y.; Li, L. Enhanced hydrogen generation via hydrolysis of Mg-Mg<sub>2</sub>NiH<sub>4</sub> system. *J. Power Sources* **2020**, *476*, 228499. [[CrossRef](#)]
18. Hou, X.; Shi, H.; Yang, L.; Hou, K.; Wang, Y.; Feng, L.; Suo, G.; Ye, X.; Zhang, L.; Yang, Y. H<sub>2</sub> generation kinetics/thermodynamics and hydrolysis mechanism of high-performance La-doped Mg-Ni alloys in NaCl solution-A large-scale and quick strategy to get hydrogen. *J. Magnes. Alloy.* **2021**, *9*, 1068–1083. [[CrossRef](#)]
19. Zheng, J.; Yang, D.; Li, W.; Fu, H.; Li, X. Promoting H<sub>2</sub> generation from the reaction of Mg nanoparticles and water using cations. *Chem. Commun.* **2013**, *49*, 9437–9439. [[CrossRef](#)] [[PubMed](#)]
20. Yuan, C.; Chen, W.; Yang, Z.; Huang, Z.; Yu, X. The effect of various cations/anions for MgH<sub>2</sub> hydrolysis reaction. *J. Mater. Sci. Technol.* **2021**, *73*, 186–192. [[CrossRef](#)]
21. Chen, J.; Fu, H.; Xiong, Y.; Xu, J.; Zheng, J.; Li, X. MgCl<sub>2</sub> promoted hydrolysis of MgH<sub>2</sub> nanoparticles for highly efficient H<sub>2</sub> generation. *Nano Energy* **2014**, *10*, 337–343. [[CrossRef](#)]
22. Hou, X.; Wang, Y.; Hu, R.; Shi, H.; Feng, L.; Suo, G.; Ye, X.; Zhang, L.; Yang, Y. Catalytic effect of EG and MoS<sub>2</sub> on hydrolysis hydrogen generation behavior of high-energy ball-milled Mg-10wt.%Ni alloys in NaCl solution-A powerful strategy for superior hydrogen generation performance. *Int. J. Energy Res.* **2019**, *43*, 8426–8438.
23. Ma, M.; Yang, L.; Ouyang, L.; Shao, H.; Zhu, M. Promoting hydrogen generation from the hydrolysis of Mg-Graphite composites by plasma-assisted milling. *Energy* **2019**, *167*, 1205–1211. [[CrossRef](#)]
24. Al Bacha, S.; Pighin, S.A.; Urretavizcaya, G.; Zakhour, M.; Castro, F.J.; Nakhil, M.; Bobet, J.L. Hydrogen generation from ball milled Mg alloy waste by hydrolysis reaction. *J. Power Sources* **2020**, *479*, 228711. [[CrossRef](#)]
25. Xie, L.; Ren, J.; Qin, Y.; Wang, X.; Chen, F.; Ba, Z. Microstructure and modified hydrogen generation performance via hydrolysis of Mg-Nd-Ni alloys. *Int. J. Hydrog. Energy* **2021**, *46*, 15288–15297. [[CrossRef](#)]
26. Jiang, J.; Ouyang, L.; Wang, H.; Liu, J.; Shao, H.; Zhu, M. Controllable Hydrolysis Performance of MgLi Alloys and Their Hydrides. *ChemPhysChem* **2019**, *20*, 1316–1324. [[CrossRef](#)] [[PubMed](#)]
27. Hou, X.; Yang, L.; Hou, K.; Shu, Q.; Cao, Q.; Liu, Y.; Feng, L.; Suo, G.; Ye, X.; Zhang, L.; et al. Hydrolysis hydrogen generation medium regulated by alkali metal cations for Mg-based alloy-Green seawater modification strategy. *J. Power Sources* **2021**, *509*, 230364. [[CrossRef](#)]
28. Pighin, S.A.; Urretavizcaya, G.; Bobet, J.L.; Castro, F.J. Nanostructured Mg for hydrogen production by hydrolysis obtained by MgH<sub>2</sub> milling and dehydriding. *J. Alloys Compd.* **2020**, *827*, 154000. [[CrossRef](#)]
29. Shao, H.; Wang, Y.; Xu, H.; Li, X. Hydrogen storage properties of magnesium ultrafine particles prepared by hydrogen plasma-metal reaction. *Mater. Sci. Eng. B* **2004**, *110*, 221–226. [[CrossRef](#)]
30. Liu, Y.; Wang, X.; Dong, Z.; Liu, H.; Li, S.; Ge, H.; Yan, M. Hydrogen generation from the hydrolysis of Mg powder ball-milled with AlCl<sub>3</sub>. *Energy* **2013**, *53*, 147–152. [[CrossRef](#)]